

DESIGN AND EXPERIMENTAL STUDY OF A SHAFTLESS DOUBLE-SCREW FERTILIZER SPREADER FOR RICE

无轴双螺旋式水稻排肥器的设计与试验研究

Ziyu WANG¹⁾; Deyu HONG¹⁾; Hongchao WANG^{*2)}; Chengyang LIU²⁾; Zanfeng MA²⁾;
Xingkang LIU²⁾; Wentao LI²⁾

¹⁾ College of Information and Electrical Engineering, Heilongjiang Bayi Agricultural University, Daqing 163319, China

²⁾ College of Engineering, Heilongjiang Bayi Agricultural University, Daqing 163319, China

Tel: 16645548678; E-mail: 452713509@qq.com

DOI: <https://doi.org/10.35633/inmateh-76-99>

Keywords: rice, spiral, fertilizer spreader, design, experiment

ABSTRACT

To address the problems of poor fertilizer distribution uniformity and low application accuracy during the operation of rice fertilizer spreaders, this paper presents the design of a shaftless double-screw fertilizer spreader for rice. Dynamic methods were combined to analyze the filling stage and discharge stage of the fertilizer spreader and to investigate the impact of its structural parameters on the uniformity of fertilizer discharge. The fertilizer distribution process was simulated using EDEM software, and single-factor experiments were conducted to analyze the effects of spiral blade outer diameter, pitch, and rotational speed on fertilizer distribution uniformity. Furthermore, a two-factor orthogonal rotational combination experiment was carried out under different structural parameter conditions to analyze the interactions between influencing factors and determine the optimal parameter combination. The optimal parameters were found to be an outer diameter of 23.3 mm, a pitch of 23.6 mm, and a rotational speed of 149.2 r/min, yielding a uniformity coefficient of variation of 6.1%. Bench test results showed that the relative error between the simulation and experimental uniformity coefficient was 0.7%, indicating strong agreement. The results meet the agronomic requirements for fertilization and ensure stable fertilizer supply. These findings provide a reference for the design optimization of spiral fertilizer spreaders.

摘要

针对水稻排肥器作业时存在施肥均匀性差和施肥精度等问题, 本文设计了一种无轴双螺旋式水稻排肥器。结合动力学方法对排肥器的充肥阶段与排肥阶段进行分析, 探究其结构参数对排肥均匀性的影响。利用 EDEM 软件对排肥过程进行仿真, 通过单因素试验分析螺旋叶片外径、螺距和螺旋转速对排肥均匀性的影响。此外, 在不同结构参数条件下进行二次正交旋转组合试验, 分析各影响因素之间交互作用并确定最佳参数组合。最优参数组合为当螺旋叶片外径为 23.3mm, 螺距为 23.6mm, 转速为 149.2r/min, 均匀性变异系数为 6.1%。台架试验结果表明: 均匀性变异系数仿真试验相对误差为 0.7%, 仿真与台架试验吻合度较好, 满足施肥农艺及供肥稳定性要求。研究结果可为螺旋式排肥器设计优化提供参考。

INTRODUCTION

Rice, as the main staple crop in China, requires efficient agricultural management practices to ensure the stability of its production and supply. Fertilization is a key agronomic practice for increasing rice yields and improving soil fertility (Qi et al., 2024). However, improper fertilization can result in yield reduction, resource waste, and environmental pollution. Precision fertilization technology enables the quantitative and accurate application of fertilizers by adjusting the operational parameters of fertilization devices, thereby significantly improving grain yield and quality while promoting sustainable agricultural development (Wang et al., 2022).

Currently, the most widely used fertilizer spreaders on the market are mainly of the external slot-wheel type and screw type, but they generally suffer from uneven fertilizer distribution, making it difficult to achieve precise and quantitative fertilization results (Yan et al., 2024). In response to these issues, researchers in China and abroad have conducted extensive studies.

Wang Jinfeng et al. (2018) analyzed improvements to the external slot wheel fertilizer spreader of a fertilizer applicator using kinematic and dynamic methods, concluding that higher rotation speeds of the fertilizer wheel are more conducive to improving distribution uniformity.

Song Cancan *et al.* (2021) designed slot wheel fertilizer distributors with different groove shapes and varying numbers of groove rows, and, through simulation and experimentation, determined reasonable structural parameters. Their results indicated that an external 4-row slot wheel achieved better performance when distributing compound fertilizer. Dun Guoqiang *et al.* (2025) designed a spiral fertilizer spreader with notched blades and analyzed the main factors affecting fertilizer uniformity using discrete element simulation and bench tests. They further optimized the parameters of the regression model through multi-objective optimization and verified the fertilization effects with different fertilizer particles. Similarly, Song Xuefeng *et al.* (2023) constructed a bonding model for fertilizer blocks using the discrete element method to examine the effects of screw rotation speed, cross-sectional shape, and screw pitch angle on the performance of a spiral groove fertilizer spreader. Fang Longyu *et al.* (2024) developed an eccentric spiral tooth fertilizer application device based on rice fertilization agronomic requirements and fertilizer particle movement patterns and conducted experiments incorporating structural parameter combinations. The results showed that the diameter of the fertilizer wheel, the number of spiral teeth, and the tooth height directly influenced device performance. Wang Yu *et al.* (2023) investigated the effects of spiral angle and installation angle on the application performance of a spiral spline drum fertilizer applicator, finding that when the spiral angle was 45° and the installation angle was 40° , the device exhibited excellent fertilization performance. Most existing studies have focused on the design optimization of sprocket structures and single-screw fertilizer spreaders, with no reported innovative designs for shaftless double-screw fertilizer spreaders. In traditional single-screw fertilizer spreaders, changes in the position of the screw blade tip at the fertilizer discharge port result in varying sizes of fertilizer storage spaces between the blade and the housing. This change has led to a periodic fluctuation in the emission of fertilizer granules, reducing the effectiveness of fertilization.

To improve the operational stability of rice fertilizer spreaders, this study proposes a shaftless double-screw fertilizer dispenser for rice, designed to meet the agronomic requirements of rice cultivation. Using EDEM, a three-factor, five-level orthogonal combination experiment was conducted to analyze the effects of spiral blade outer diameter, pitch, and rotational speed on fertilizer discharge performance. Based on the experimental results, the structural parameters of the dispenser were optimized, and bench tests were performed to further verify its operational performance.

MATERIALS AND METHODS

Main structure and working principle of the shaftless double-screw fertilizer spreader

The shaftless double-screw fertilizer spreader consists primarily of end covers, drive gears, spiral blades, and a housing (Fig. 1). Two sets of shaftless double-screw blades are arranged in parallel inside the spreader, forming a continuous material-conveying plane. The housing adopts an inverted “8”-shaped cavity design, ensuring that the screw blades remain in close contact with the housing. This configuration effectively reduces fertilizer residue and promotes stable material flow.

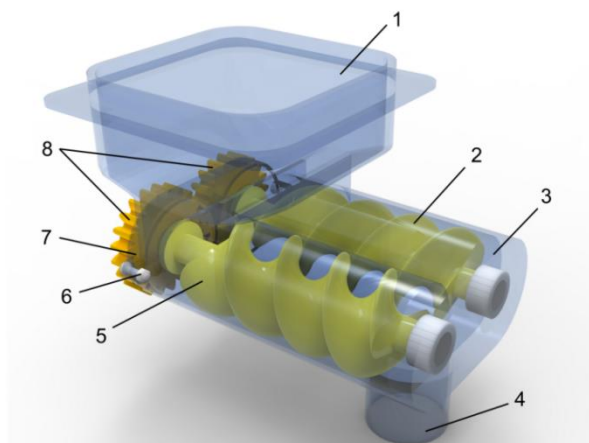


Fig. 1 - The experimental bench for synchronized corn seeding and precision hole fertilization

1. feed inlet; 2. left-hand spiral blade; 3. housing; 4. discharge outlet; 5. right-hand spiral blade; 6. bolt; 7. end cover; 8. drive gear.

The fertilizer spreader is mounted at the bottom of the hopper. During operation, fertilizer enters the housing through the feed port. Power from the tractor is transmitted via the drive shaft to the gearbox, which drives the two sets of spirals to rotate at the same speed but in opposite directions. Under the combined action of the dual spiral blades, layered advancement and dynamic mixing of fertilizer particles are achieved.

The continuous rotation of the blades generates axial thrust, pushing the fertilizer toward the discharge port. The phase-complementary motion of the dual spirals eliminates the periodic fluctuations typically observed in single-screw fertilizer spreaders, thereby ensuring uniform material conveyance. Finally, the fertilizer is evenly delivered to the discharge port through the coordinated action of the dual spirals and discharged via the outlet piping.

Modeling of fertilizer loading and discharge dynamics

Mechanical analysis of the fertilizer loading stage

The fertilizer loading stage is the critical process in which fertilizer particles are transferred from the hopper into the housing and undergo initial filling. At the beginning of this stage, the particles in the hopper are in a piled state. When the spiral mechanism is activated, the particles are propelled forward by the combined effects of gravity, the thrust generated by the dual spiral blades, and interparticle forces during blade rotation. The force analysis of fertilizer particles is illustrated in Figure 2.

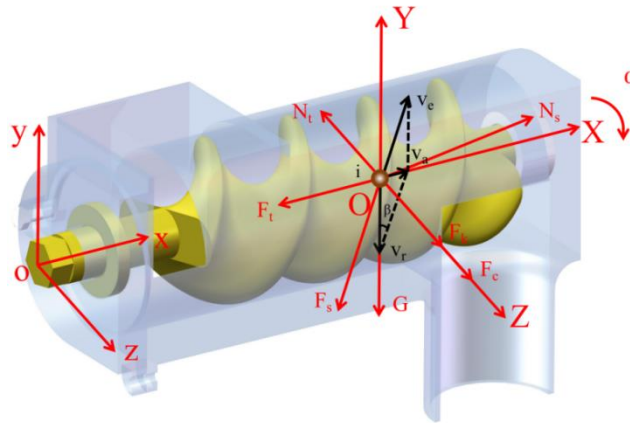


Fig. 2 - The force analysis of fertilizer particles

As shown in Figure 2, a fixed reference frame O-XYZ is established with the spiral shaft axis aligned with the X-axis and the opposite direction of gravity aligned with the Y-axis. A moving reference frame o-xyz, rotating periodically with the spiral blades, is also defined. Ignoring the interaction between adjacent particles, the motion trajectory of a representative particle i during the filling stage can be observed.

The dynamic equilibrium equation for the particles can be expressed as:

$$G + N_s + F_s + F_c + N_t + F_t + F_k = mg + N_s + \mu N_s + m\omega^2 R + m\omega^2 R + \mu N_t + 2m\omega v_i = 0 \quad (1)$$

where G is the gravitational force acting on fertilizer particle i during the fertilization process (N); N_s is the normal support force of the spiral surface (N); F_s is the sliding friction force on the spiral surface (N); F_c is the centrifugal inertial force (N); N_t is the support force from the wall of the fertilizer discharge pipe (N); F_t is the friction force of the fertilizer discharge pipe (N); F_k is the Coriolis inertial force (N); m is the mass of a single fertilizer particle (kg); ω is the angular velocity of the shaftless double spiral blade (rad/s); R is the distance from the center of mass of particle i to the Y-axis (m); μ is the friction coefficient between particle i and the surface of the shaftless double spiral blade; v_i is the relative velocity between particle i and the outer edge of the screw blade (m/s); v_a is the absolute velocity of particle i (m/s); v_c is the relative velocity of particle i (m/s); v_t is the entrainment velocity of particle i (m/s); and β is the helix angle of the screw blade ($^\circ$).

The X components of the sliding friction force (F_s), normal support force (N_s), and fertilizer discharge pipe friction force F_t are shown in Equation (2).

$$F_s \sin \beta + F_t = N_s \cos \beta \quad (2)$$

The Y components of the gravitational force G , normal support force N_s , and sliding friction force F_s are shown in Equation (3).

$$G + F_s \cos \beta = N_s \sin \beta \quad (3)$$

The Z-components of the drag inertia force F , fertilizer discharge pipe support force N_t , and Coriolis force F_k are shown in Equation (4).

$$F_k + F_C = N_t \quad (4)$$

Combining equations (1) to (4), equation (5) is obtained.

$$\begin{cases} \mu N_s \sin \beta + \mu m \omega^2 R = N_s \cos \beta \\ mg + \mu N_s \cos \beta = N_s \sin \beta \\ 2m\omega v_i + m\omega^2 R = N_t \end{cases} \quad (5)$$

In practical operation, the relative velocity v_e of the particles is small, and thus the Coriolis force F_k can be neglected. Setting $F_k \approx 0$ simplifies the expression to Equation (6).

$$R = \frac{mg(\cos \beta - \mu \sin \beta)}{\mu m \omega^2 (\sin \beta - \mu \cos \beta)} \quad (6)$$

In summary, according to Equation (6), the motion of fertilizer particles during the fertilization process is influenced by the angular velocity of the shaftless spiral blade, the distance from the particle's center of mass to the Y-axis, and the helix angle of the spiral surface.

Kinematic model of the fertilizer discharge stage

During the fertilizer discharge stage, when fertilizer particles detach from the spiral blades and fall into the fertilizer discharge pipe, their velocity is equal to the tangential velocity of the spiral blades (v_R). Under the combined effects of their own gravity, centrifugal and inertial forces, and air resistance (F_f), the particles fall into the fertilizer discharge pipe, performing a projectile motion with a parabolic trajectory as shown in Figure 3.

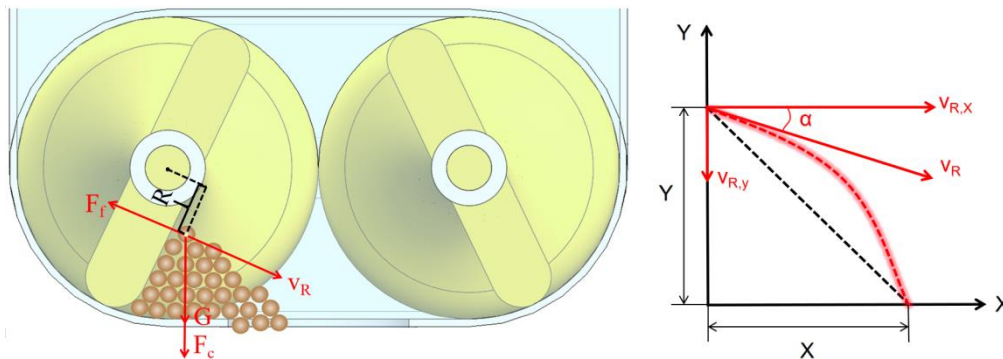


Fig. 3 - The force analysis of fertilizer particles

The tangential velocity of the spiral blades is the product of the distance from the center of mass of the fertilizer particles to the spiral axis and the angular velocity of the spiral blades.

$$v_R = \omega R \quad (7)$$

The components in the X-axis and Y-axis directions are shown in Equation (8).

$$v_{R,x} = v_R \cos \alpha \quad (8)$$

$$v_{R,y} = v_R \sin \alpha \quad (9)$$

where α is the angle between the tangential velocity of the spiral blades and the horizontal direction, °.

According to Newton's second law, the differential equation of motion for the inclined projectile motion of fertilizer is established, as shown in Equation (10).

$$\begin{cases} m \frac{d^2 x}{dt^2} = 0 \\ m \frac{d^2 y}{dt^2} = mg \end{cases} \quad (10)$$

where m is the mass of the fertilizer particle, kg; x is the displacement of the fertilizer particle in the X-axis direction, m; y is the displacement of the fertilizer particle in the Y-axis direction, m.

At this point, the equation of motion for the fertilizer is shown in Equation (11).

$$\begin{cases} x = v_R \cos \alpha \cdot t \\ y = v_R \sin \alpha \cdot t + \frac{1}{2} g t^2 \end{cases} \quad (11)$$

The trajectory equation is given by Equation (12).

$$y = x \tan \alpha + \frac{g}{2\omega^2 R^2 \cos^2 \alpha} x^2 \quad (12)$$

From Equation (12), although increasing the rotational speed can enhance the tangential velocity, it also intensifies the centrifugal effect, causing particles to aggregate toward the outer edge and potentially disrupting the uniformity of filling. During actual fertilizer discharge, it is necessary to optimize the spiral outer diameter and rotational speed to make most particles approach a certain average value, thereby balancing centrifugal force and conveying efficiency.

Structural Design

From the analysis of the working process of the spiral fertilizer spreader, it can be concluded that the parameters most significantly affecting its fertilization performance are the outer diameter (D), the pitch (S), and the rotational speed (n). The main geometric parameters of the fertilizer supply spiral are shown in Figure 4.

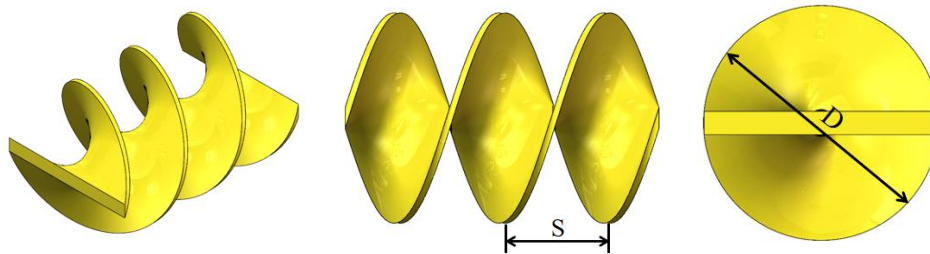


Fig. 4 - The main geometric parameters of the fertilizer supply spiral

The outer diameter of the spiral blades, as the core parameter of the spiral fertilizer spreader, directly influences fertilizer output, operational stability, and power consumption. Its design should be determined comprehensively by considering material characteristics, agronomic requirements, and structural constraints. Based on empirical formulas and literature data, the quantitative relationship between the target fertilizer output (Q) and the outer diameter of the spiral blades can be expressed as shown in Equations (13)–(15).

$$Q = 47 K_1 A \phi \lambda \varepsilon D^{\frac{5}{2}} \quad (13)$$

$$K = \left(\frac{1}{47 K_1 A} \right)^{\frac{5}{2}} \quad (14)$$

$$D \geq K \left[\frac{Q}{\phi \lambda \varepsilon} \right]^{\frac{2}{5}} \quad (15)$$

where K is the characteristic coefficient of the fertilizer particles; K_1 is the ratio coefficient of pitch to diameter; A is the comprehensive characteristic coefficient of the material; ϕ is the filling coefficient; λ is the unit volume mass of the material (t/m^3); ψ is the filling coefficient; ε is the spiral inclination angle coefficient.

Considering the agronomic requirements for fertilization in the Heilongjiang region, the influence of the screw structure volume on the fertilizer discharge rate, and stability concerns at high discharge speeds (Wang et al., 2018), the standard integer series of screw conveyor diameters was calculated. As a result, the design range for the screw blade outer diameter D was adjusted to 18–44 mm.

The pitch size not only determines the helix angle but also affects the slip surface morphology and velocity distribution of fertilizer movement under a given filling coefficient, thereby directly influencing the continuity and stability of material conveyance (Xu et al., 2024). The selection of an appropriate pitch requires comprehensive consideration of the frictional characteristics between the screw surface and the material, as well as the compatibility of the velocity components. The pitch is typically determined using the empirical formula in Equation (16).

$$D \geq K \left[\frac{Q}{\phi \lambda \varepsilon} \right]^{\frac{2}{5}} \quad (16)$$

where K_1 is a coefficient, typically ranging from 0.8 to 1.0. In this design, since the shaftless spiral blades are arranged parallel to the horizontal plane, and based on existing experience and comprehensive analysis, K_1 is set to 0.9. Consequently, the pitch range is determined to be 16.2–39.6 mm.

With a fixed screw shaft structure, adjustment of the fertilizer discharge volume is often achieved by changing the rotational speed. Increasing the rotational speed increases the discharge volume; however, it must be kept within a reasonable range. Excessively high speeds can cause fertilizer particles to be thrown outward by centrifugal force, resulting in discharge blockage, reduced filling time, a lower filling coefficient, and deterioration of discharge stability. Therefore, it is necessary to ensure that the inertial centrifugal force acting on the fertilizer particles does not exceed their gravitational force, thereby preventing particles from scattering outward and failing to be conveyed properly.

$$n_{\max} = \frac{30K\sqrt{2g}}{\pi\sqrt{D}} \quad (17)$$

$$A = \frac{30K\sqrt{2g}}{\pi} \quad (18)$$

$$n_{\max} = \frac{A}{\sqrt{D}} \quad (19)$$

where K_0 is the comprehensive material property coefficient; n_{\max} is the maximum rotational speed of the screw conveyor; A is the comprehensive material property coefficient. For granular fertilizers, A is taken as 28, resulting in a calculated range for the actual rotational speed of the screw blades of 134–209 r/min.

Simulation model and parameter settings

To investigate the fertilizer distribution performance of a shaftless double-screw fertilizer spreader, simulation experiments were conducted using the Rocky–DEM discrete element software (Sugirbay *et al.*, 2020). To improve computational efficiency, secondary structural components that do not meet fertilizer particles were removed from the shaftless double-screw fertilizer spreader model, retaining only the core functional components. A simplified three-dimensional model was constructed in SolidWorks, comprising five main components: the fertilizer hopper, double-screw blades, housing, end caps, and fertilizer collection trough. The model was then exported in STL format and imported into Rocky-DEM. The simulation model of the shaftless double-screw fertilizer spreader is shown in Figure 5.

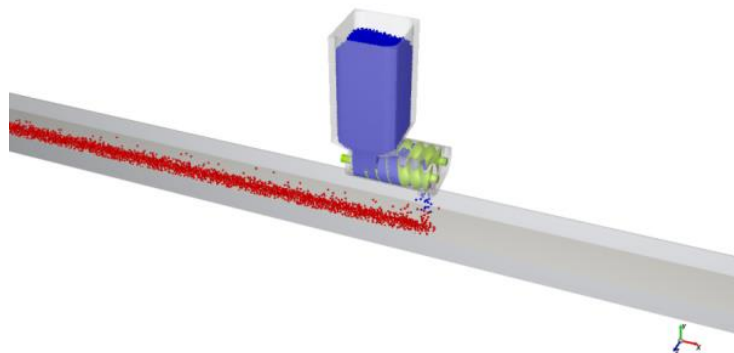


Fig. 5 - Simulation model of the shaftless double-screw fertilizer spreader

The core working principle of the shaftless double-screw fertilizer spreader is based on the dynamic contact and interaction between fertilizer particles and the rotating spiral blade surfaces, the particles and the housing cavity walls, and between the particles themselves. In this study, the Hertz–Mindlin (no slip) contact model and the Linear Spring Coulomb Limit model were selected to describe the normal and tangential contact forces, thereby accurately representing particle collisions and simulating the actual operating environment of the spreader. Referring to relevant literature and experimental methods, actual fertilizer particles were sampled

and measured ($n = 100$). The particle size distribution was found to follow a normal distribution, with an average diameter of 3.28 mm and a standard deviation of 0.41 mm. For the purposes of simulation, the fertilizer particle model was simplified to a perfect sphere, and the particle density was set to 1670 kg/m³ based on measured values. According to the experimental measurement results, the parameters are set as shown in Table 1.

Table 1

Parameters required for discrete element simulation		
Item	Property	Value
Fertilizer particles	Poisson's ratio	0.25
	Shear modulus (Pa)	1.0×10^7
	Density (kg/m ³)	1670
PLA plastic	Poisson's ratio	0.3
	Shear modulus (Pa)	4.0×10^8
	Density (kg/m ³)	1255
Particle to particle	Recovery factor	0.52
	Static friction coefficient	0.48
	Rolling friction coefficient	0.28
Particle to discharging wheel and shell	Recovery factor	0.51
	Static friction coefficient	0.23
	Rolling friction coefficient	0.18

Experimental design

A total of 5 kg of fertilizer granules were generated in the fertilizer box using the volume filling method and filled uniformly within 1 s to simulate the fertilizer filling process (Tian et al., 2024). Once all particles were generated, the shaftless double-screw blades were started at a preset speed, while the fertilizer dispenser moved at a speed of 0.20 m/s along a straight line to simulate the operating conditions of a rice transplanting machine. The discharged fertilizer particles fell into a fertilizer collection trough with a width of 100 mm and a length of 2000 mm. The specific calculations were performed according to the following formulas.

$$\bar{X} = \frac{\sum_{i=1}^{m_0} X_i}{m_0} \quad (20)$$

$$\bar{Y} = \frac{\sum_{i=1}^{m_0} Y_i}{m_0} \quad (21)$$

$$\sigma = \sqrt{\frac{\sum_{i=1}^{m_0} (X_i - \bar{X})^2}{m_0 - 1}} \quad (22)$$

$$V = \frac{\sigma}{\bar{X}} \times 100\% \quad (23)$$

Where:

m is the number of measurements; Y_i is the total fertilizer discharge volume for each test, g; \bar{Y} is the average stability of the total fertilizer discharge volume for each test, g; X_i is the mass of fertilizer particles in the i -th grid, g; \bar{X} is the average mass of fertilizer particles in all grid units; σ is the standard deviation between grid cells, g; V is the coefficient of variation of fertilizer uniformity between individual grid cells, %.

Based on the grid method principle, 10 equally spaced grid units were set up in the stable operating section of the conveyor belt, with each grid unit measuring 100 mm × 100 mm. The specific configuration of the simulated mass statistical grid is shown in Figure 6 (Sugirbay et al., 2020). After calculating the fertilizer mass within each grid, the mean stability and coefficient of variation of uniformity were determined (Chen et al., 2021).

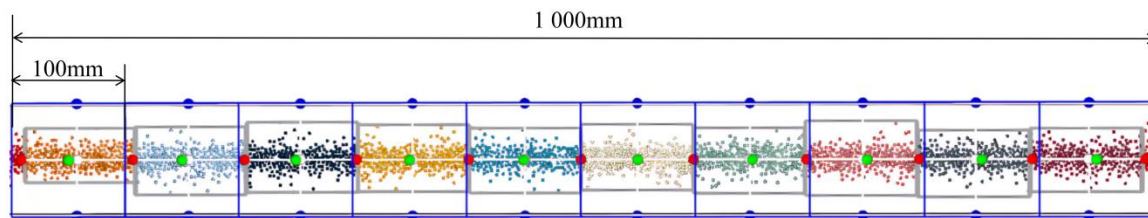


Fig. 6 - The specific configuration of the simulated mass statistical grid

Three sets of single-factor experiments were designed. Under fixed conditions of spiral blade outer diameter (42 mm) and pitch (30 mm), the performance was tested at six rotational speed levels: 140, 155, 170, 185, 200, and 215 r/min. Second, under fixed pitch (30 mm) and rotational speed (180 r/min) conditions, performance was tested at six levels of diameter: 18, 24, 30, 36, 42, and 48 mm. Under fixed rotational speed (180 r/min) and diameter (42 mm) conditions, the performance was tested at six levels of lead: 16, 22, 28, 34, 40, and 46 mm.

The mean stability of fertilizer application rate and the coefficient of variation of fertilizer application uniformity were used as experimental evaluation indicators, and a quadratic regression orthogonal rotated combination experiment was conducted (Chen *et al.*, 2021). The factor level coding table is shown in Table 2.

Table 2

The factor level coding

Coded value	Factor		
	The outer diameter (mm)	The pitch (mm)	The rotational speed (r/min)
1.682	44	39.6	209
1	38.7	34.9	193.8
0	31	27.9	171.5
-1	23.3	20.7	149.2
-1.682	18	16.2	134

RESULTS AND DISCUSSIONS

Effect of spiral blade outer diameter on fertilizer distribution performance

As shown in Figure 7, the experimental results indicate that as the outer diameter of the spiral blades increases, the coefficient of variation of uniformity gradually decreases, with the overall range of variation in the uniformity coefficient spanning from 2.56% to 14.85%. Additionally, as the spiral blade outer diameter increases, the mean stability value progressively increases, showing a strong linear correlation. The goodness of fit, $R^2 = 0.98$, indicates a high level of accuracy. Therefore, precise fertilization can be achieved by adjusting the outer diameter of the spiral blades.

Effect of pitch on fertilizer distribution performance

As shown in Figure 8, the experimental results indicate that as the pitch of the spiral blades increases, the coefficient of variation of uniformity exhibits fluctuating changes. Specifically, the coefficient of variation initially decreases gradually, then increases, reaching a peak near a pitch of 32 mm, and subsequently shows a decreasing trend. The coefficient of variation reaches a maximum of 12.32% and a minimum of 3.46%. Additionally, as the pitch of the spiral blades increases, the mean stability value generally increases, although it decreases between 34 mm and 40 mm.

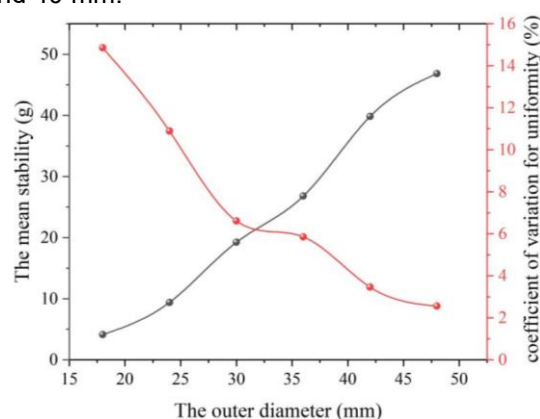


Fig. 7 - Effect of spiral blade outer diameter on fertilizer distribution performance

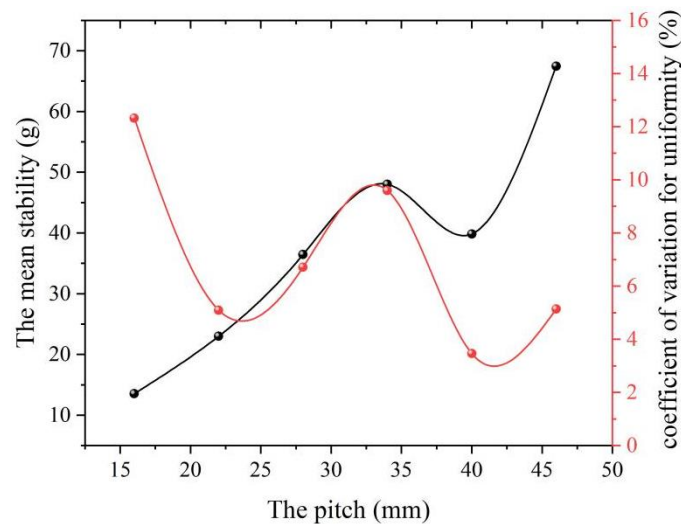


Fig. 8 - Effect of pitch on fertilizer distribution performance

Effect of rotational speed on fertilizer distribution performance

As shown in Figure 9, the experimental results indicate that as the rotational speed of the spiral blades increases, the coefficient of variation of uniformity first decreases, with the overall range of variation being 5.44% to 14.33% between 185 and 220 r/min. Additionally, as the screw blade speed increases, the mean stability value gradually increases, exhibiting a good linear relationship with a high degree of fit ($R^2 = 0.97$). This suggests that precise fertilizer application can be achieved by adjusting the screw speed.

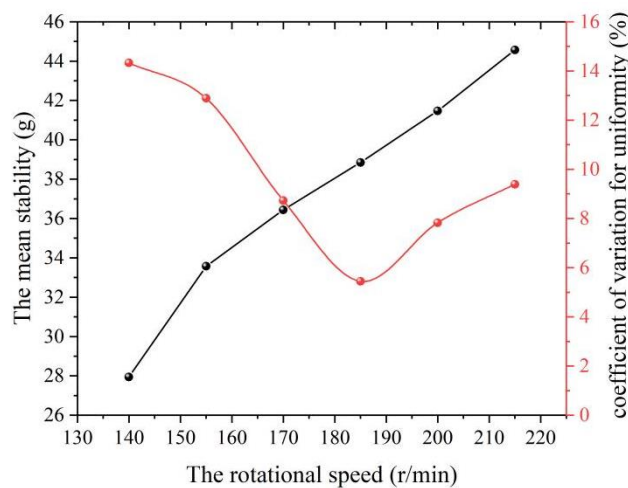


Fig. 9 - Effect of rotational speed on fertilizer distribution performance

Multi-factor Parameter Optimization Analysis

The coefficient of variation for uniformity is a key indicator for evaluating fertilizer performance. Therefore, this study focuses on analyzing the effects of interaction between various factors on the coefficient of variation for uniformity. After performing multiple regression analysis using Design-Expert 8.0.6 software, regression equations for each factor's influence on the coefficient of variation for uniformity were derived (Adilet *et al.*, 2023). The results of the analysis of variance (ANOVA) and significance are shown in Table 3. All regression equations were highly significant ($P < 0.01$). Additionally, the P-value for misfit was not significant, indicating that the equations fit well. In the ANOVA results for the coefficient of variation of uniformity, the P-value for misfit was 0.59, indicating that no other factors had an influence. Under the conditions that all models are significant and the misfit term is not significant, the insignificant factors are removed, and the factor coded value regression equation is established, as shown in Equation (24).

$$y_1 = -3.78 - 0.26x_3 - 0.03x_1x_2 - 0.03x_1^2 + 0.03x_2^2 \quad (24)$$

where:

y_1 is the coefficient of variation of uniformity, %; x_1 is the outer diameter of the spiral blade, mm; x_2 is the pitch of the spiral blade, mm; x_3 is the rotational speed of the spiral blade, r/min.

Table 3

The results of the analysis of variance for the regression equations

Source of variance	Coefficient of variation for uniformity (%)			
	Square sum	Degrees of freedom	F	P
Model	169.27	9	5.72	0.0026**
x_1	0.0168	1	0.0051	0.9441
x_2	7.31	1	2.22	0.1598
x_3	40.19	1	12.22	0.0039*
x_1x_2	15.70	1	4.78	0.0478*
x_1x_3	0.0010	1	0.0003	0.9863
x_2x_3	2.53	1	0.7702	0.3961
x_1^2	61.62	1	18.74	0.0008*
x_2^2	21.49	1	6.54	0.0239*
x_3^2	1.14	1	0.3459	0.5665
Residual	42.74	13		
Lost proposal	14.07	5	0.7853	0.59
Errors	28.67	8		
Sum of all	212.01	22		

Note: * indicates significant ($P < 0.05$) and ** indicates highly significant ($P < 0.01$).

Figure 10 shows the effect of rotational speed and pitch on the coefficient of variation for fertilizer uniformity under the condition of a spiral blade outer diameter of 31 mm. As indicated in the figure, when the rotational speed remains constant, the coefficient of variation first decreases and then increases as the pitch gradually increases. This suggests that there is an optimal pitch range within which fertilizer uniformity is maximized. A pitch that is too small may cause material blockage or unstable output, while a pitch that is too large can lead to a discontinuous fertilization rhythm, thereby reducing uniformity. On the other hand, when the pitch is fixed, the coefficient of variation increases monotonically with increasing rotational speed, implying that higher rotational speeds weaken the stability and uniformity of fertilization. This could be due to high-speed rotation causing the fertilizer to be ejected too quickly, which hinders uniform distribution and may lead to material jumping or intermittent flow issues (Wang *et al.*, 2022).

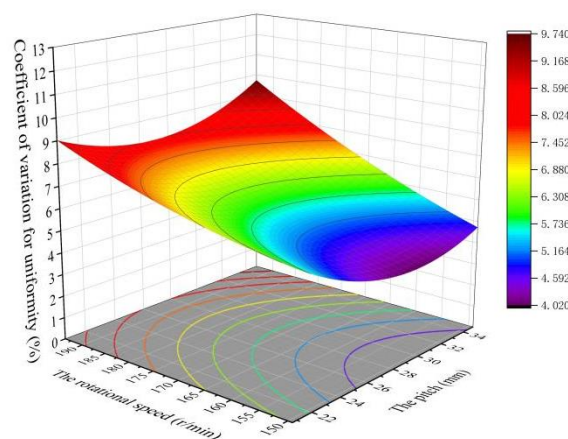


Fig. 10 - Effect of rotational speed and pitch on the coefficient of variation for uniformity

Figure 11 illustrates the effects of pitch and outer diameter on the coefficient of variation of uniformity under a spiral blade rotational speed of 171.5 r/min. The figure clearly shows the distinct influence patterns of the two parameters on fertilizer application uniformity. When the pitch remains constant, the coefficient of variation increases and then decreases as the spiral blade outer diameter increases. In contrast, when the outer diameter remains constant, the coefficient of variation continuously increases as the pitch increases. This indicates that while a larger pitch may increase the fertilizer application rate per unit time, it is more likely to cause intermittent or concentrated material output during transmission, disrupting the stability of fertilizer application and thus reducing uniformity.

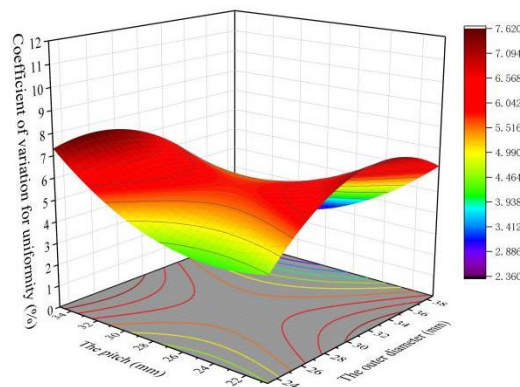


Fig. 11 - Influence of pitch and outer diameter on the coefficient of variation for uniformity

Figure 12 shows the relationship between rotational speed and outer diameter on the coefficient of variation of uniformity, with the pitch fixed at 27.8 mm. As can be seen from the figure, when the rotational speed remains constant, the coefficient of variation of uniformity first increases and then decreases as the outer diameter of the spiral blades increases. Additionally, under fixed outer diameter conditions, as the rotational speed increases, the coefficient of variation shows a continuous upward trend, indicating that higher rotational speeds are more likely to cause unstable material dispersion and disordered distribution, which negatively impacts fertilizer uniformity.

To determine the optimal parameter combination, boundary conditions must be set and a mathematical model established using software (Dun et al., 2021). The mathematical model obtained through analysis is given in Equation (25).

$$\begin{cases} \min y_1 \\ s.t. \begin{cases} 18\text{mm} \leq x_1 \leq 44\text{mm} \\ 16.2\text{mm} \leq x_2 \leq 39.6\text{mm} \\ 134\text{r/min} \leq x_3 \leq 209\text{r/min} \end{cases} \end{cases} \quad (25)$$

Optimization using the Design-Expert optimization module yields the following optimal combination: spiral blade outer diameter of 23.3 mm, pitch of 23.6 mm, and rotational speed of 149.2 r/min, resulting in a uniformity coefficient of variation of 5.64%. Simulation verification of the optimized parameters yielded a uniformity coefficient of variation of 6.1%, which is in good agreement with the optimization results. To verify the fertilizer supply performance of the fertilizer dispenser, bench tests were conducted on the shaftless double-screw fertilizer spreader, as shown in Figure 13. The bench test was conducted using the optimal parameter combination, with the average value taken from three repeated experiments. The measured coefficient of variation for uniformity was 6.7%, differing by 0.6% from the simulation results. The deviation may be attributed to measurement errors in manual measurements and the impact of vibrations during the test process on fertilizer supply performance. Nevertheless, the fertilizer supply performance met the agronomic requirements.

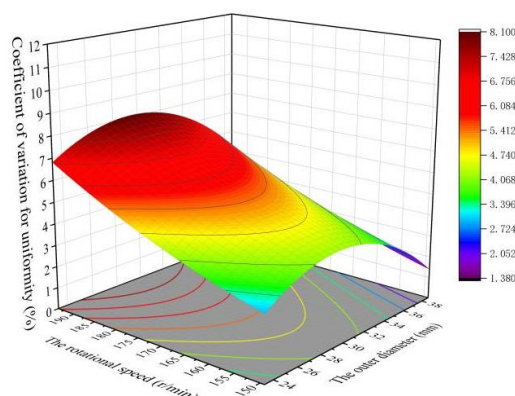


Fig. 12 - Influence of rotational speed and outer diameter on the coefficient of variation for uniformity

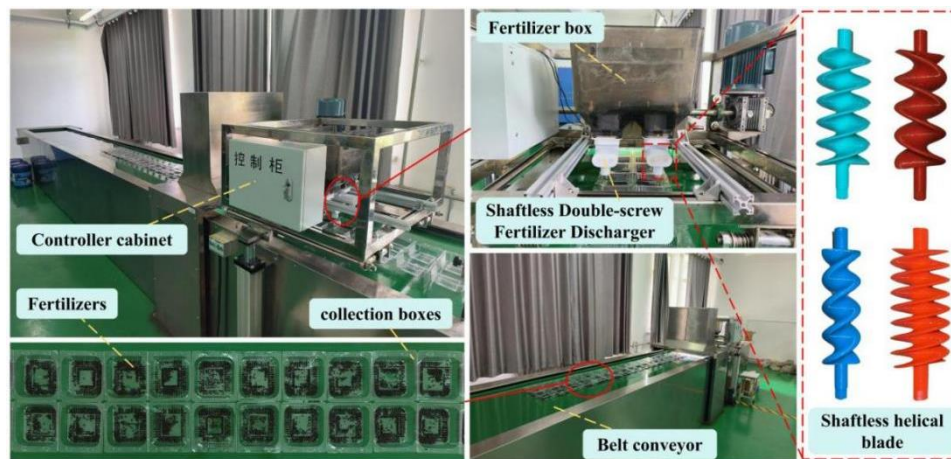


Fig. 13 - Bench test of the shaftless double-screw fertilizer spreader

CONCLUSIONS

This paper designs a shaftless double-helix rice fertilizer spreader and conducts a theoretical analysis of its fertilizer supply performance to identify the primary factors influencing its performance. Single-factor simulation test results indicate that the outer diameter, pitch, and rotational speed of the spiral blades all affect fertilizer distribution. By reasonably adjusting the outer diameter, pitch, and rotational speed of the spiral blades, a precise fertilizer supply can be achieved.

A quadratic regression orthogonal rotation combination experiment was conducted. Using Design-Expert software, variance and response surface analysis were performed on the results of the orthogonal rotation combination experiment. The results indicate that the regression equations are highly significant ($P < 0.01$). Optimization of the fertilization performance indicators was performed. When the outer diameter of the spiral blades was 23.3 mm, the pitch was 23.6 mm, and the rotational speed was 149.2 r/min, simulation results indicated a uniformity coefficient of variation of 6.1%. Bench verification tests showed a uniformity coefficient of variation of 6.7%, demonstrating that fertilization performance met agronomic requirements.

ACKNOWLEDGEMENT

This research was funded by the China Postdoctoral Science Foundation, grant number 2024MD763975; the School Orientation Training Research Initiation Fund Program, grant number XYB202307; the Heilongjiang Provincial Postdoctoral General Funding Project, grant number LBH-Z24250; the National Key Research and Development Program, grant number 2016YFD0200600.

REFERENCES

- [1] Adilet S., Zhao K., Liu G., Sayakhat N., Chen J., Hu G., Marat M. (2023). Investigation of the pin-roller metering device and tube effect for wheat seeds and granular fertilizers based on DEM. *International Journal of Agricultural and Biological Engineering*, 16(2), 103–114. <https://doi.org/10.25165/j.ijabe.20231602.7721>
- [2] Chen H., Zheng J., Lu S., Zeng S., Wei S. (2021). Design and experiment of vertical pneumatic fertilization system with spiral Geneva mechanism. *International Journal of Agricultural and Biological Engineering*, 14(3), 135–144. doi:10.25165/j.ijabe.20211404.6575
- [3] Dun G., Gao Z., Liu Y., Ji W., Mao N., Wu X., Liu W. (2021). Optimization design of fertilizer apparatus owned arc gears based on discrete element method. *International Journal of Agricultural and Biological Engineering*, 14(2), 97–105. <https://doi.org/10.25165/j.ijabe.20211402.5719>
- [4] Dun G., Sheng Q., Ji X., Li H., Ma C., Li X., Sun H., Wang L., Ma C., Wang H. (2025). Parameter optimization of the notched blade spiral fertilizer discharger for pineapple orchards based on DEM. *Frontiers in Mechanical Engineering*, 11, 1535013. <https://doi.org/10.3389/fmech.2025.1535013>
- [5] Fang L., Yang W., Luo X., Guo H., Song S., Liu Q., Li G. (2024). Development and optimization of an offset spiral tooth fertilizer discharge device. *Agriculture*, 14(2), 329. <https://doi.org/10.3390/agriculture14020329>
- [6] Qi Z., Liu C., Wang Y., Zhang Z., Sun X. (2024). Design and experimentation of targeted deep fertilization device for corn cultivation. *Agriculture*, 14(9), 1645. <https://doi.org/10.3390/agriculture14091645>

- [7] Song C., Zhou Z., Wang G., Wang X., Zang Ying. (2021). Optimization of the groove wheel structural parameters of UAV-based fertilizer apparatus. *Transactions of the Chinese Society of Agricultural Engineering*, 37(22), 1–10. <https://doi.org/10.11975/j.issn.1002-6819.2021.22.001>
- [8] Song X., Dai F., Zhang X., Gao W., Li X., Zhang F., Zhao, W. (2023). Simulation and experiment of fertilizer discharge characteristics of spiral grooved wheel with different working parameters. *Sustainability*, 15(14), 118309. <https://doi.org/10.3390/su151411309>
- [9] Sugirbay A., Zhao J., Nukeshev S., Chen J. (2020). Determination of pin-roller parameters and evaluation of the uniformity of granular fertilizer application metering devices in precision farming. *Computers and Electronics in Agriculture*, 179, 105835. <https://doi.org/10.1016/j.compag.2020.105835>
- [10] Tian L., Li H., Zhang X., Liu, C. (2024). Discrete Element Method simulation of rice grain stacking characteristics. *INMATEH Agricultural Engineering*, 74(3), 554-561. <https://doi.org/10.35633/inmateh-74-49>
- [11] Wang J., Gao G., Weng W., Wang J., Yan D., Chen B. (2018). Design and Experiment of Key Components of Side Deep Fertilization Device for Paddy Field. *Transactions of the Chinese Society for Agricultural Machinery*, 49(6), 92–104. <https://doi.org/10.6041/j.issn.1000-1298.2018.06.011>
- [12] Wang J., Wang Z., Weng W., Liu Y., Fu Z., Wang, J. (2022). Development status and trends in side-deep fertilization of rice. *Renewable Agriculture and Food Systems*, 37(5), 550–575. <https://doi.org/10.1017/s1742170522000151>
- [13] Wang Y., Tan Y., Wei S., Liao M., Zang, Y., Zeng, S. (2023). Design and experimental study of the fertilizer applicator with vertical spiral fluted rollers. *International Journal of Agricultural and Biological Engineering*, 16(5), 80–87. <https://doi.org/10.25165/ijabe.20231605.7555>
- [14] Yan S., Zhong W., Wu G., Bai X., Di J., Zhao X. (2024). Optimisation and testing of structural parameters of internal tangent circle external grooved wheele fertiliser discharger. *INMATEH Agricultural Engineering*, 74(3), 895–907. <https://doi.org/10.35633/inmateh-74-79>
- [15] Xu W., Yuan Q., Zeng J., Lü X. (2024) Design and experiment of four-head inclined spiral precision fertilizer dischargers in orchard. *Transactions of the Chinese Society for Agricultural Machinery*, 55(s2), 30–40. <https://doi.org/10.6041/j.issn.1000-1298.2024.S2.004>